PREDICTING THE EFFECT OF A FOREST CANOPY ON GROUND SNOW PACK ACCUMULATION AND ABLATION IN MARITIME CLIMATES.

Pascal Storck[1], Dennis P. Lettenmaier[1]

ABSTRACT

To investigate the processes controlling snow accumulation and ablation beneath forest canopies in maritime climates, continuous measurements of snow water equivalent (SWE) and snowpack outflow were made during the winters of 1996/97 and 1997/98 at a site in the transient snow zone of the Southern Oregon Cascades. Measurements were taken with large weighing lysimeters (~25 m^2) below a mature canopy and in an adjacent harvested site. Analysis of the observations shows that approximately 60% of annual snowfall was intercepted by the canopy (up to an apparent maximum above 30 mm), with approximately 72 percent removed as meltwater drip and 28 percent removed as large snow masses. Apparent sublimation rates from the intercepted snow were less than 1 mm per day. These data, along with measurements of standard micrometeorology, were used to develop and test an energy balance model of snow interception and canopy effects on ground snowpack ablation. The model represents intercepted snow load as a function of Leaf Area Index, adjusted for the effects of temperature. Removal of intercepted snow by sublimation, melt-water drip and mass release is governed by available energy, the vapor pressure deficit, and the liquid water content of the intercepted snow. The profiles of wind and radiation through the canopy are modeled explicitly. Turbulent heat exchange at the surface is calculated via the bulk aerodynamic method and corrected for atmospheric stability via a modified Richardson's number approach. The model was calibrated to the 1996/97 observations and validated using the 1997/98 data. Model predictions of snow accumulation at both sites are highly sensitive to the rain/snow threshold temperature while predicted ablation agrees well with observations.

INTRODUCTION

Considerable attention has been given to quantifying changes in energy flux to the snow surface due to forest canopy removal in the Pacific Northwest (e.g. Berris and Harr 1987, Beaudry and Golding 1983). These studies have demonstrated that enhancement of near surface wind, temperature and radiation influences ground snow pack ablation rates. Less understood, although equally important in controlling total water delivery to the soil during a melt event, are those processes in the forest canopy that control ground snow pack accumulation. Although several studies in maritime climates have collected data and described models of snow interception (see Hedstrom and Pomeroy (1998) for a brief review), these data and models are limited in their description of the intercepted snow's fate.

More recent advances in data collection and process model development have been reported for cold climates (e.g. Hedstrom and Pomeroy 1998, Lundberg et al. 1998). Most of these models include explicit representations for the growth of intercepted snow and its removal via sublimation and unloading (as parcels of snow). However, these data do not completely describe processes in temperate maritime environments where melt of intercepted snow can be significantly more important than either sublimation or unloading. An understanding of snow interception, sublimation, melt and mass release is critical to developing a predictive model of ground snowpack dynamics relevant to such regions, including the Pacific Northwest. This paper describes a field campaign to investigate these processes along with an energy balance model of intercepted and ground snow pack dynamics developed as a direct consequence of the field investigation.

EXPERIMENTAL DESIGN

A series of experiments were carried out in the transient snow zone (1200 m) of the southern Oregon Cascades (50 km NW of Crater Lake) during the winters of 1996/97 and 1997/98 as part of the Demonstration of Ecosystems Management Options (DEMO) Project. A detailed discussion of the snow hydrology component of DEMO is given in Storck et al. (1999).

[1]Dept of Civil and Environmental Engineering, Box 352700, University of Washington, Seattle, WA 98195

Annual precipitation at the field site is on the order of 2 meters, 70% of which falls between October and April. First snowfall typically occurs in late October. Significant snow accumulation usually begins in late November. In clearings, snow cover is generally present throughout the winter with average maximum water equivalents of approximately 350 mm. Average winter temperatures are often near freezing. The snowpack is maintained throughout the winter by occasional heavy snowfalls. Mid-winter melt is common and is driven mainly by turbulent heat fluxes. Final melt occurs in late April or early May. The location of the site near the Cascade Crest exposes it to frequent rain-on-snow (ROS) events as well as a pronounced radiation-dominated melt season each spring. Mature forest stands at the site range in age from 110-130 years. The canopy is dominated by Douglas-fir (*Pseudotsuga menziesii*). Average tree heights approach 40 meters.

To investigate ground snow pack accumulation and ablation, large weighing lysimeters (Figure 1) were installed. Snow interception and canopy dynamics can be inferred by comparing the data from the two beneath-canopy lysimeters (each with a surface area of 25 m^2) to that from an adjacent shelterwood (surface area of 12.5 m^2). The mature canopy site has canopy characteristics similar to those described above with an average canopy closure of approximately 80%. The shelterwood site has a 15% random canopy retention. Each lysimeter is weighed continuously by load cells and outflow is measured by 1-liter capacity tipping buckets buried below grade to prevent freezing. Each beneath-canopy lysimeter is installed around a Douglas-Fir tree to ensure 100% canopy coverage over the lysimeter. The large surface area of the beneath-canopy lysimeter effectively removes the variability due to preferential flowpaths of canopy throughfall by sampling at the scale of a single tree's canopy. Standard micrometeorology data (air temperature, humidity, windspeed, precipitation) were collected at all sites as well as incoming short- and long-wave radiation.

Figure 1. Overview of beneath-canopy weighing lysimeters. Each lysimeter is installed around a mature Douglas-Fir tree. A precipitation gauge is shown in the foreground.

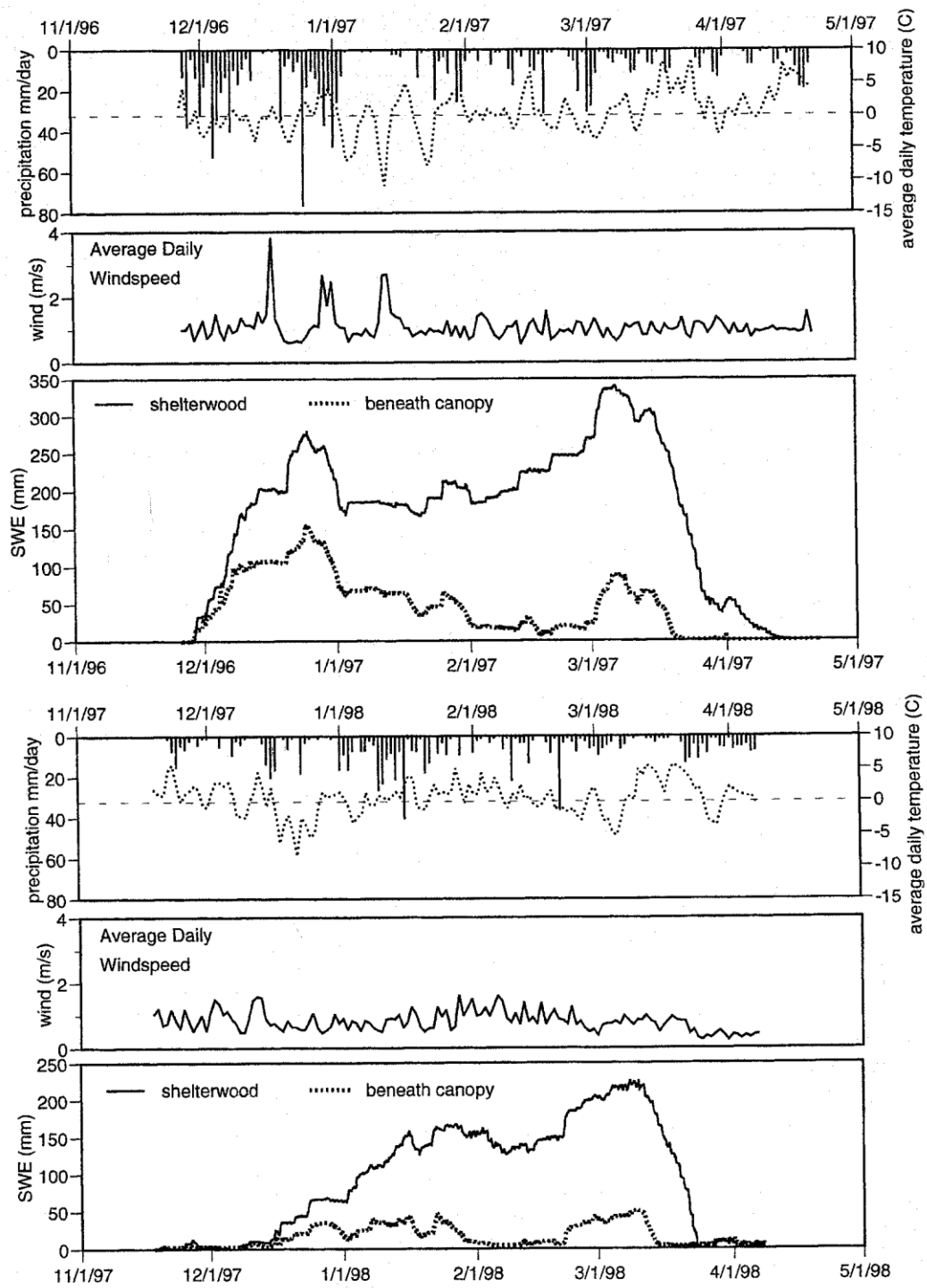

Figure 2. Observed accumulation and ablation of snow water equivalent over two snow seasons by the shelterwood and beneath-canopy weighing lysimeters. Daily average windspeed and air temperature are also shown for each season along with total daily precipitation.

DATA

The data collection effort serves as the foundation of the model development described below. Therefore, a brief overview of the observed data for the winters of 1996/97 and 1997/98 is included here. Additional details regarding data collection are provided in Storck et al. (1999).

Figure 2 shows observed beneath-canopy and shelterwood SWE for both seasons as well as daily precipitation and average daily air temperature and wind speed. The overall effect of the forest canopy in reducing ground snow accumulation is dramatic, and clearly is not well described by a simple relationship between "beneath-canopy" and "open" snow accumulation. For example, during the period through 1-Jan 1997, snow interception processes limited overall accumulation to approximately 50% of the shelterwood value. Even more dramatic is the period from 10- Jan 1997 to 1- Mar 1997 during which snow continued to accumulate at the shelterwood site but did not beneath the canopy. Equally impressive differences in snow accumulation due to the forest canopy occurred during the 1997/98 season.

While these data reveal large differences in seasonal snow accumulation due to the forest canopy, they also provide information about the growth of intercepted snow in the canopy and its ultimate fate. Figure 3 shows apparent snow interception during 24 individual snowfall events from 1996 to 1998. Snow interception is inferred as the difference between snow accumulation observed by the shelterwood and beneath-canopy lysimeters immediately after snowfall ends. In all events, interception is approximately 60% of total snowfall and can exceed 30 mm of water equivalent. Although not shown on figure 3, snow interception during events was approximately 60% at all times during snowfall, providing evidence for a linear snow interception growth function.

Comparisons between lysimeter data also provide estimates of losses due to the mature canopy. Figure 4 shows the SWE plus accumulated outflow for the shelterwood and beneath-canopy lysimeters. Net loss is the residual of total SWE plus outflow at both sites and provides an estimate of overall sublimation/evaporation loss from the canopy. Estimated annual sublimation is on the order of 100 mm and is strongly dependent on local micrometeorology. During the relatively cold (-5°C<T<0°C) period from 12/1/1997 to 12/31/1997, estimated sublimation is 34 mm (~1 mm/day). However, during the warm, wet period from 1/1/98 to 1/16/98, apparent sublimation was limited to 4 mm due to rapid removal of snow from the canopy via meltwater drip and mass release.

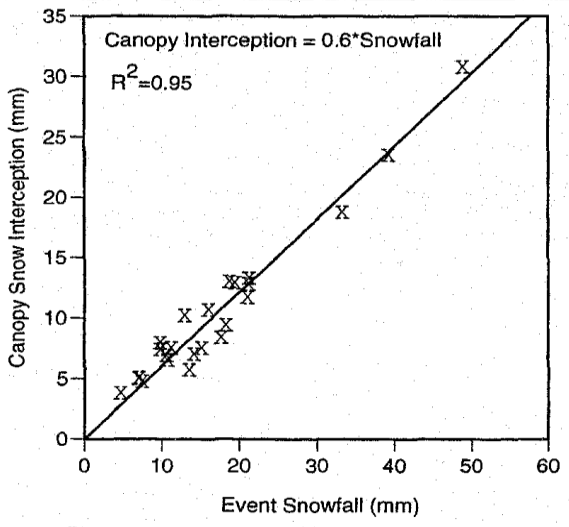

Figure 3. Estimated snow interception by a mature Douglas-Fir canopy (residual of open and below canopy snow accumulation) for 24 snowfall events.

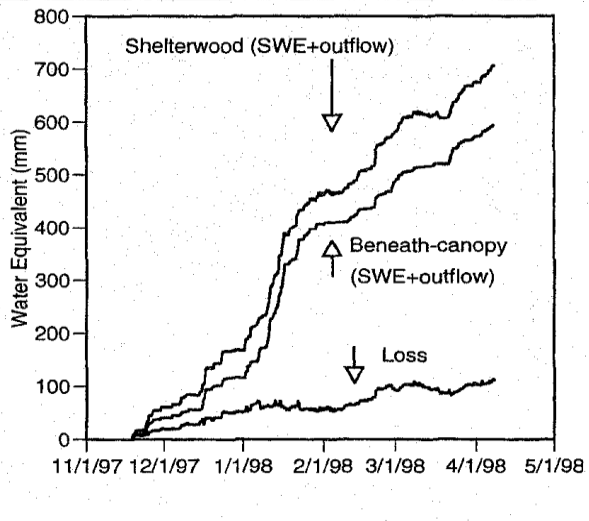

Figure 4. Estimated sublimation loss from intercepted snow (residual of shelterwood and beneath-canopy total water)

Evidence for the relative magnitudes of meltwater drip, mass release and sublimation can be obtained from the period from 1-Dec 1996 to 14-Dec 1996 during which neither melt of the ground snowpack nor rainfall occurred (i.e. canopy processes controlled ground snow dynamics). Snow accumulation in the shelterwood was 195 mm, while only 111 mm accumulated beneath the canopy, a difference of 84 mm. During this same time period, snowpack outflow beneath the canopy was exactly 84 mm greater than in the shelterwood, suggesting that sublimation of intercepted snow was negligible. Assuming that 60% of all snowfall was intercepted by the canopy, these data imply that only 28% (33 mm) of intercepted snow reached the ground as snow while 72% (84 mm) was removed as meltwater drip.

MODEL FORMULATION

Snowpack energy balance

To model snow interception and snowpack dynamics, an energy balance approach is used (see e.g., Anderson 1976). The ground snowpack is modeled as two layers, a thin surface layer and the pack layer, while intercepted snow is modeled as a single layer. Energy exchange between the atmosphere, forest canopy and snowpack occurs only with the surface layer. The energy balance of the surface layer is

$$\rho_w c_s \frac{dWT_s}{dt} = Q_r + Q_s + Q_e + Q_p + Q_m \qquad (1)$$

where c_s is the specific heat of ice, ρ_w is the density of water, W is the water equivalent of the snowpack surface layer , T_s is the temperature of the surface layer, Q_r is the net radiation flux, Q_s is the sensible heat flux, Q_e is the latent heat flux, Q_p is the energy flux given to the snowpack via rain or snow, and Q_m is the energy flux given to the pack due to liquid water refreezing or taken from the pack during melt.

Except for differences in the formulation of the atmospheric stability correction to the turbulent heat fluxes (discussed briefly below), the energy balance of the ground snow pack is almost identical to formulations presented elsewhere (Anderson 1976, Jordan 1991, Marks 1992) and details are not provided here.

The flux of sensible heat to the snow surface is given by:

$$Q_s = \frac{\rho c_p (T_a - T_s)}{r_a} \qquad (2)$$

$$r_a = \frac{\ln\left[\frac{z - d_s}{z_o}\right]^2}{k^2 U_z} \qquad (3)$$

where ρ_a is air density, c_p is the specific heat of air, T_a is the air temperature and r_a is the aerodynamic resistance between the snow surface and the near-surface reference height (z). In Eq. 3, k is von Karman's constant, z_o is the snow surface roughness, d_s is the snow depth, U is wind speed and z is the near-surface reference height. Similarly, the flux of latent heat to the snow surface is given by:

$$Q_e = \frac{\lambda_i \rho \left[\frac{0.622}{P_a}\right]\left[e(T_a) - e_s(T_s)\right]}{r_a} \qquad (4)$$

where λ_i is the latent heat of vaporization when liquid water is present in the surface layer and the latent heat of sublimation in the absence of liquid water, P_a is atmospheric pressure, e and e_s are the vapor and saturation vapor pressure respectively.

The calculation of turbulent energy exchange (Q_s, Q_e) is complicated by the effect of atmospheric stability. During snowmelt, the atmosphere immediately above the snow surface is typically warmer than the snow surface. As parcels of cooler air near the snow surface are transported upward via turbulent eddies they tend to sink back toward the surface and turbulent exchange is suppressed. Aerodynamic resistance can be corrected for atmospheric stability as indexed by the bulk Richardson's number (Ri_b) (e.g. Anderson 1976)

$$Ri_b = \frac{gz(T_a - T_s)}{\frac{(T_a + T_s)}{2} U(z)^2} \qquad (5)$$

with the correction for stable conditions given as

$$r_a = \frac{r_a}{(1-\frac{Ri_b}{Ri_{cr}})^2} \qquad 0 \le Ri_b < Ri_{cr} \tag{6}$$

and in unstable conditions as

$$r_a = \frac{r_a}{(1-16Ri_b)^{0.5}} \qquad Ri_b < 0 \tag{7}$$

where Ri_{cr} is the critical value of the Richardson's number (commonly taken as 0.2) at which turbulent exchange is completely suppressed under stable conditions.

While the bulk Richardson's number correction has the advantage of being straightforward to calculate based on observations at only one level above the snow surface, previous investigators have noted that it completely suppresses turbulent exchange under common melt conditions and usually leads to an underestimation of the latent and sensible heat fluxes to the snowpack (e.g. Jordan 1991, Tarboton 1995). Therefore, a correction to the above stability formulation is used (Storck et al. 1997), which is based on a comparison of the above formulation to an alternative scheme based on mixing length theory (e.g. Marks 1992). The net effect of this correction is that the maximum value of Ri_b is limited by:

$$Ri_b = \min(Ri_b, \frac{1}{\ln(\frac{z}{z_o})+5}) \tag{8}$$

Snow interception model

During each time step, snowfall is intercepted by the canopy according to

$$I = f\,S \tag{9}$$

where I is the water equivalent of snow intercepted during a time step, S is the snowfall rate and f is the efficiency of snow interception (60% in Figure 3). The maximum interception capacity (B) is given by

$$B = L_r(m * LAI) \tag{10}$$

where LAI is the leaf area index of the canopy and m is determined based on observations of maximum snow interception capacity. The leaf area ratio (L_r) is a step function of temperature:

$$L_r = 0.004 \qquad T_a > -5^0 C \tag{11}$$

$$L_r = 0.001 \qquad T_a \le -5^0 C \tag{12}$$

based on observations by Kobayashi (1987) that snow interception efficiency decreases rapidly as the air temperature decreases below -3°C.

Newly intercepted rain (R) is calculated with respect to the water holding capacity of the intercepted snow (W_c), which is given by the sum of the capacity of the snow and bare branches:

$$W_c = hC + 1e^{-4}(LAI) \tag{13}$$

where h is the water holding capacity of snow (taken as approximately 3.5%). Excess rain becomes throughfall.

Fate of intercepted snow

The intercepted snow pack can contain both ice and liquid water. The mass balance for each phase is:

$$\Delta C = I - M + \left[\frac{Q_e}{\rho_w \lambda_s} + \frac{Q_m}{\rho_w \lambda_f}\right]\Delta t \tag{14}$$

$$\Delta W = R + \left[\frac{Q_e}{\rho_w \lambda_v} - \frac{Q_m}{\rho_w \lambda_f}\right]\Delta t \tag{15}$$

where M is snow mass release from the canopy, and λ_s, λ_v, λ_f are the latent heat of sublimation, vaporization and fusion, respectively. Snowmelt is calculated directly from a modified energy balance, similar to that applied for the ground snow pack, in which

$$T_s = \min(T_a, 0) \tag{16}$$

The modification arose during testing of a fully iterative (on T_s) intercepted snow energy balance, which revealed that the intercepted snow temperature never departed significantly from the air temperature. Snowmelt in excess of

the liquid water holding capacity results in meltwater drip (D). Mass release of snow from the canopy occurs if sufficient snow is available and is related linearly to the production of meltwater drip:

$$M = 0 \qquad C < n \tag{17}$$

$$M = 0.4D \qquad D \geq 0 \tag{18}$$

where n is the residual intercepted snow which can only be melted (or sublimated) off the canopy (taken as 5 mm in model testing). The ratio of 0.4 in Eq. 18 is derived from observations of the ratio of mass release to meltwater drip (as discussed above, M/D = 33 / 84 = 0.4).

MODEL TESTING

The model was calibrated against the shelterwood (adjusting T_{min}, T_{max}, and z_o) and beneath-canopy (adjusting k and z_o) weighing lysimeter data for the 1996/97 snow year. At values between T_{min} and T_{max}, the model assumes a mixture of rain and snow occurs which is linearly dependent on air temperature. For both the calibration and validation periods, only micro-meteorological observations from the shelterwood site were used to force the model. Air temperature, humidity, precipitation, incoming short- and long-wave radiation in the shelterwood were assumed to be good approximations of above-canopy conditions. Wind speed at the 2-m (above soil) measurement height in the shelterwood was corrected for snow accumulation beneath the anemometer and then scaled to the 80-m height assuming a logarithmic profile and a surface roughness of 1 cm. The energy balance of intercepted snow was driven with above canopy forcings while aerodynamic resistance was calculated by Eq. 3 using the 80-m wind, canopy displacement height (0.65*H) and canopy roughness (0.1*H) where H is the height of the canopy.

Below-canopy shortwave radiation was taken as 16% of the above-canopy value based on observations. Below-canopy windspeed was adjusted to match observations (i.e. 25% of shelterwood value). Below canopy longwave (L_c) was calculated via:

$$L_c = (1 - F)L_o + (F) * \sigma(T_a)^4 \tag{19}$$

where L_o is above canopy longwave and F is the average stand level canopy coverage (80%). Air temperature and humidity were assumed identical at the shelterwood and below-canopy sites. A comparison of the observed and predicted below-canopy meteorological values is shown in Figure 5 for a ROS and radiation-dominated event.

Both the shelterwood and mature sites collect large amounts of forest liter (needles, moss, etc), therefore snow albedo was assumed to decay with age. Based on observations in the shelterwood site (see Figure 5d):

$$\alpha_a = 0.85(\lambda_a)^{t^{0.58}} \tag{20}$$

$$\alpha_m = 0.85(\lambda_m)^{t^{0.46}} \tag{21}$$

where α_a and α_m are the albedo during the accumulation and melt seasons, t is the time in days since the last snow, λ_a is 0.92, and λ_m is 0.7.

Model results

Table 1 lists the parameters that yielded the best fit calibration shown in Figure 6a. Accumulation and ablation of SWE are well predicted at both sites. Best agreement with observed values occurs when the below canopy snow surface roughness is 20 times larger than the shelterwood values. Although an upper maximum on canopy snow interception is not apparent from the observed data, a $m*LAI$ of 10 provided the best agreement with observations. Decreasing $m*LAI$ resulted in significant overestimation of below-canopy SWE, while increasing $m*LAI$ did not change predictions of SWE. These results suggest an upper maximum on canopy interception of 40 mm SWE.

Table 1. Parameter values from snow model calibration to a shelterwood and mature site (1996/97 data).

site	parameter	value
Shelterwood	T_{min} (for rain)	-1.0 °C
Shelterwood	T_{max} (for snow)	0.5 °C
Shelterwood	z_0	0.01 (m)
Beneath-canopy	$m*LAI$	10
Beneath-canopy	z_0	0.20 (m)

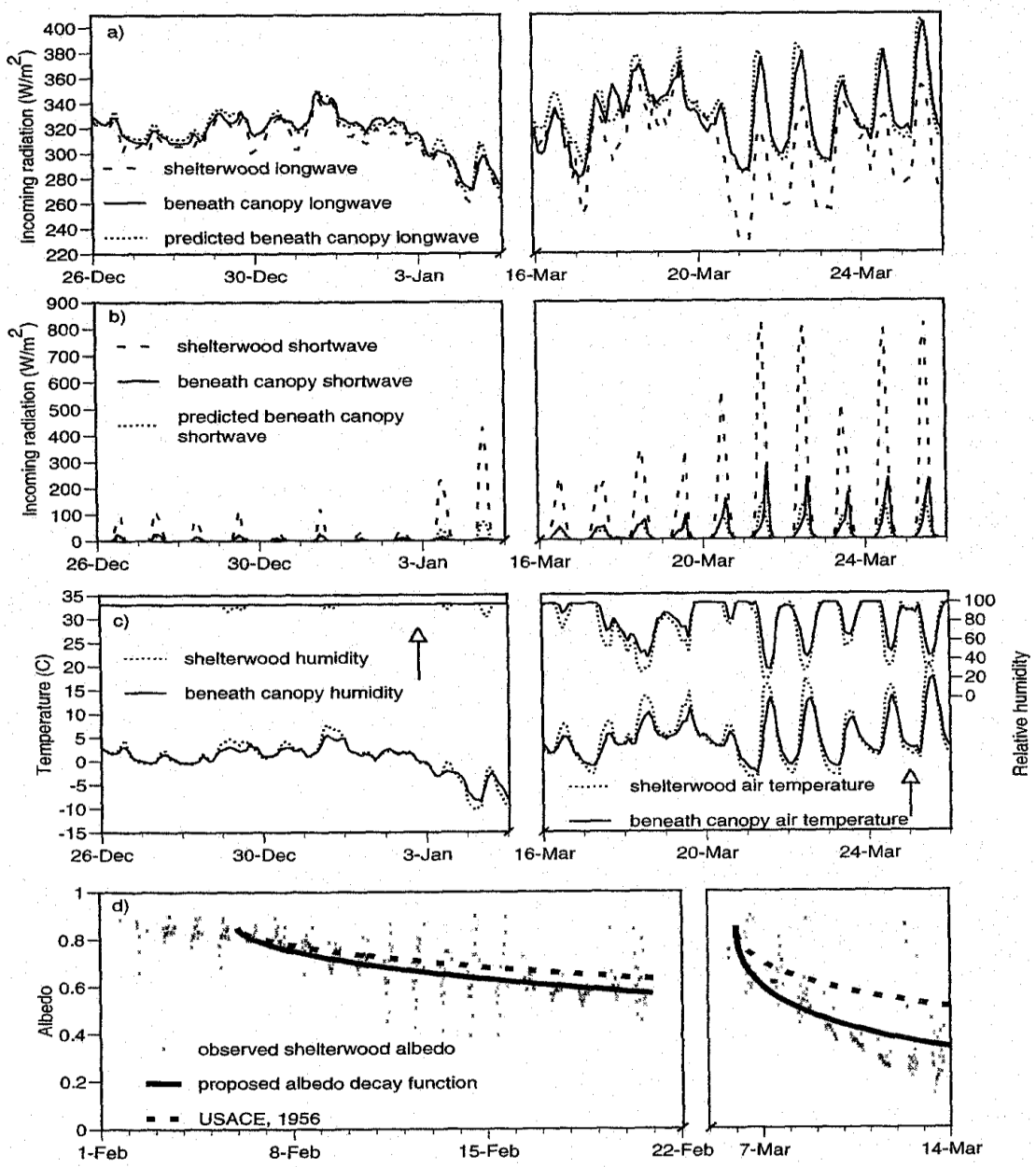

Figure 5. Observed beneath-canopy and shelterwood meteorology for a major ROS event (26-Dec 1996 to 5-Jan 1997) and a spring melt event (16-Mar to 26-Mar, 1996) a) observed longwave radiation at both sites vs. predicted beneath-canopy, b) observed shortwave radiation at both sites vs. predicted beneath-canopy, c) observed air temperature and relative humidity at both sites, and d) observed decay of snow albedo during two snow free periods.

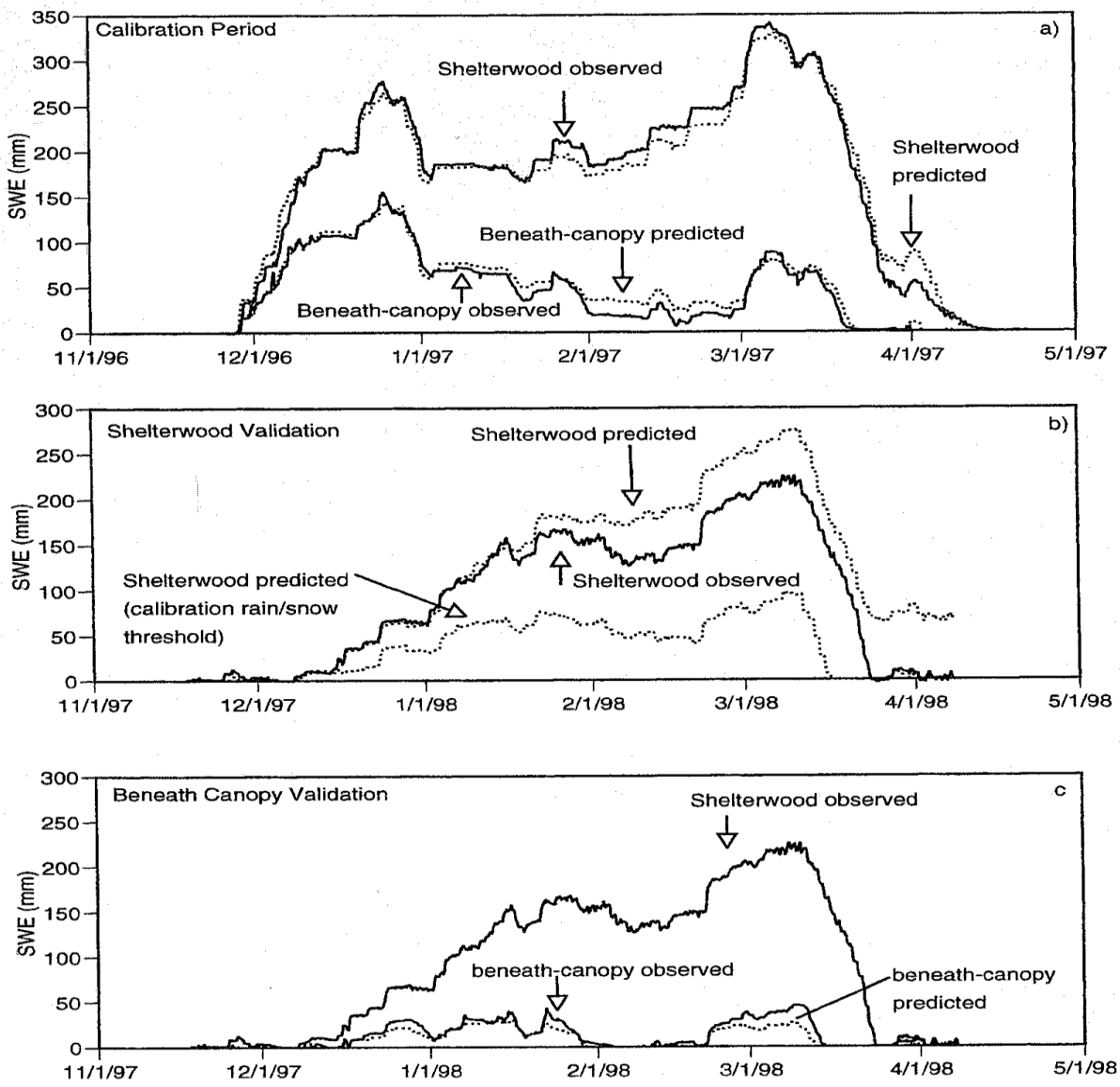

Figure 6. Results of a) full canopy snow model calibration to 1996/97 weighing lysimeter data, b) validation against 1997/98 shelterwood data, and c) validation against 1997/98 beneath-canopy data. Note the two predicted SWE simulations for the shelterwood validation (Figure 6b). The lower curve uses a rain/snow threshold of (-1.0, 0.5) (identical to the calibration period (Figure 6a)) while the upper curve uses (0.4, 0.5). Subsequent validation against the beneath canopy data uses (0.4, 0.5) as the rain/snow threshold.

Figure 6 b shows the validation of the model against the 1997/98 shelterwood weighing lysimeter data. Given the calibration threshold rain-snow temperatures, SWE is significantly underestimated, especially during the initial accumulation phase. Adjusting the rain and snow threshold to 0.4 °C and 0.5 °C, respectively, yielded the best agreement with observations. This change also caused considerable over-prediction of late season SWE due to the continual accumulation of snow from 1-Feb 1998 to 20-Feb 1998 (which was not observed on the lysimeter). Ironically, the best fit for the late season snow accumulation was obtained with the original rain-snow threshold values (-1.0, 0.5). Given that 1997/98 was a strong El-Nino year, a time dependent rain-snow threshold may be defensible, but in the absence of observations of the form of precipitation such a time dependant threshold simply becomes an exercise in curve fitting. Therefore, the higher rain-snow threshold was adopted for the beneath-canopy simulations. Figure 6c shows the validation of the below canopy snow model. Given sufficient snow at the shelterwood site, beneath-canopy SWE accumulation and ablation were quite well predicted.

Limited sensitivity analysis of ground snowpack model

Figure 7a shows the sensitivity of the 1996/97 shelterwood SWE predictions to the albedo formulation. As expected, the formulation based on local measurements of albedo results in significantly better predictions than the formulation based on the measurements of USACE (1956).

Figures 7b and 7c show the sensitivity of the below canopy SWE prediction to the stability formulation. In Figure 7b, the limited stability correction (adopted in this paper) is compared to the unrestricted formulation. Allowing the turbulent heat fluxes to be completely suppressed leads to underestimation of melt rates and overestimation of SWE. Since an unrestricted stability correction and a surface roughness of 20 cm result in insufficient melt, one could argue that a simple increase in surface roughness could lead to an equally acceptable calibration with the unrestricted formulation. However, this is not the case. Figure 7b shows that if the surface roughness is increased from 20 cm to 40 cm, the model overestimates snowmelt during the New Year's ROS event. However, it underestimates subsequent melt events (most notably on Feb. 1 and Feb. 15). This argues for simultaneously decreasing roughness for the New Year's event and increasing it for later events, which is the net effect achieved by the restricted formulation.

Figure 7c shows a similar attempt to recalibrate the "no correction" model. With a snow surface roughness of 20 cm and no stability correction, melt is significantly overestimated. If the snow surface roughness is reduced to 5 mm, melt rates under the canopy are still overestimated. Further reduction of snow surface roughness beneath the canopy is not justified.

CONCLUSIONS

Based on the observed data, several conclusions can be drawn regarding snow interception and its ultimate fate in maritime climates.

1) Snow interception in a maritime climate is an important process with interception efficiency as high as 60% of snowfall and maximum interception capacities of over 30 mm SWE.

2) Under cold conditions, sublimation can be an important mechanism for removal of intercepted snow with seasonal rates near 1 mm per day. However, under warm conditions (which are more prevalent, especially in the transient snow zone), meltwater drip and mass release dominate sublimation with meltwater drip accounting for the removal of up to 70% of intercepted snow.

3) A simple energy balance model of snow interception and its fate can accurately predict seasonal below-canopy snow accumulation.

ACKNOWLEDGEMENTS

The model formulation presented in this paper is based on field data collected as a part of the Demonstration of Ecosystem Management Options project. Our colleagues in the data collection part of this endeavor are Travis Kern and Susan Bolton, both from the College of Forest Resources, University of Washington. This work was also supported, in part, by a NASA Earth Systems Science fellowship to the first author.

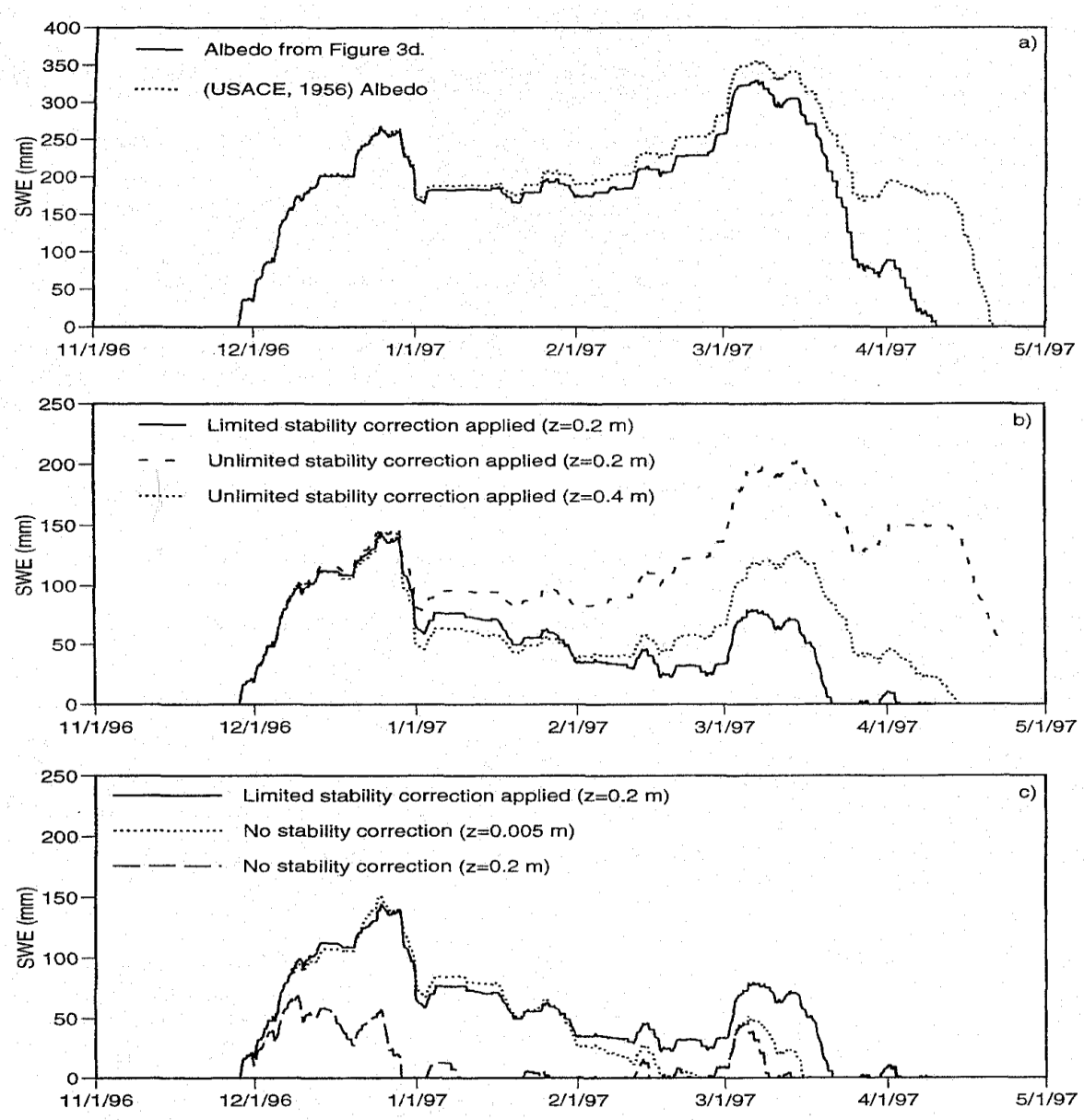

Figure 7. Sensitivity of ground snow pack to albedo and stability formulation. a) Sensitivity analysis of albedo formualtion on shelterwood snow ablation, b) comparison of limited stability formualtion to unlimted formualtion, and c) comparison of limited stability formulation to assumption of constant neutral stability.

REFERENCES

Anderson, E. A., A point energy and mass balance model of a snow cover, *NWS Technical Report 19*, National Oceanic and Atmospheric Administration, Washington, DC. 150 pp, 1976.

Beaudry, P. G., and D. L. Golding, Snowmelt during rain-on-snow in coastal British Columbia, in *Proc. 51th Western Snow Conf..*, pp. 55-66, Colorado State University, Fort Collins, 1983.

Berris, S. N., and R. D. Harr, Comparative snow accumulation and melt during rainfall in forested and clear-cut plots in the western Cascades of Oregon, *Water Resources Research*, **23**(1), 135-142, 1987.

Hedstrom, N. R., and J. W. Pomeroy, Measurement and modelling of snow interception in the boreal forest, *Hydrological Processes*, **12**, 1611-1625, 1998.

Jordan, R., A one-dimensional temperature model for a snow cover: technical documentation for SNTHERM.89, *Special Report 91-16*, US Army Corps of Engineers Cold Regions Research and Engineering Laboratory, Hanover, NH, 49 pp., 1991.

Kobayashi, D., Snow accumulation on a narrow board, *Cold Regions Sc. Technol.*, **13**, 239-245, 1987.

Lundberg, A., Ian Calder, I., and R. Harding, Evaporation of intercepted snow: measurement and modelling. *Journal of Hydrology*, **206**, 151-163, 1998.

Marks, D., and J. Dozier, Climate and energy exchange at the snow surface in the alpine region of the Sierra Nevada: 2. Snow cover energy balance, *Wat. Resour. Res.*, **28**, 3043-3054, 1992.

Storck, P., B. Nijssen, and D. P. Lettenmaier, The effect of the atmospheric stability formulation on snow accumulation and melt in mature forests, *EOS Trans AGU*, Fall Meeting Suppl., 1997.

Storck, P., Kern, T., and S. Bolton, Measurement of differences in snow accumulation and ablation due to forest harvesting, *Northwest Science*, 73, 87-101, 1999.

Tarboton, D. G., T. G. Chowdhury, and T. H. Jackson, A spatially distributed energy balance snowmelt model, in Tonneson, K. A., W. Williams, and M. Tranter (eds), Biogeochemistry of Seasonally Snow Covered Catchments, *IAHS-AIHS Publication 228*, International Association of Hydrological Sciences, Wallingford, pp. 141-155, 1995.

US Army Corps of Engineers (USACE), Snow Hydrology: Summary report of the snow investigations, North Pacific Division, Portland, Oregon. 437 pp., 1956.